Detectability by Electromagnetic Sounding Systems

RAJNI K. VERMA

Abstract—**An analysis has been made of the detectability of subsurface layers by the four electromagnetic (EM) depth sounding systems: horizontal coplanar loops, perpendicular loops, vertical coplanar loops, and vertical coaxial loops. For computing the mutual coupling ratios (the EM response function) the linear digital filter method has been used. The linear digital filter method as applied in computing the EM fields has been briefly reviewed. The EM sounding systems have been compared for the relative effectiveness in the mapping of subsurface inhomogeneities.**

Introduction

ELECTROMAGNETIC (EM) depth sounding methods have been developed quite recently with rapid advancement of the EM theory. The EM sounding methods are now an important means of investigating the layered earth structures. Major applications are in petroleum exploration, ground water exploration (especially in arid zones), geothermal resources exploration, and foundation engineering. The three commonly employed sources for generating the EM fields in geophysical exploration are loops of wire, short grounded lengths of wire, and long grounded lengths of wire. A small current-carrying loop of wire generates the magnetic field which cannot be distinguished from that caused by a dipole magnet provided that the field is observed at a distance of about five times the diameter of the loop.

The loops may be oriented in any arbitrary direction with respect to the surface of the earth. The systems for EM soundings considered here are as follows:

1) horizontal coplanar loops;
2) perpendicular loops;
3) vertical coplanar loops;
4) vertical coaxial loops.

With these systems, the voltage proportional to the current in the source is measured, rather than a magnetic field. The theoretical curves and the field data are given in terms of the mutual coupling ratio (Z/Z_0). The ratio of the received voltage to source current is Z, which is the mutual coupling between the source and the receiver. Z_0 is the free-space mutual coupling computed for the primary field. A detailed description of the manner of and a more complete definition of mutual coupling ratio are given by Frischknecht [1].

Considerable work has been done for determination of the EM fields over a conducting earth. Wait [2], [3] has developed expressions for the mutual coupling ratios of loops over a homogeneous and a two-layer earth. Frischknecht [1] has tabulated the mutual coupling ratios for horizontal coplanar, perpendicular, vertical coplanar, and vertical coaxial loop configurations on and above a two-layer ground by numerical integration of the infinite integrals involved on a digital computer; displacement currents are neglected. Dey and Ward [4] and Ryu *et al.* [5] have given formal solutions for loops placed on a multilayered earth with displacement currents having been taken into consideration. Lajoie *et al.* [6] have given a new computational approach for computing the EM response of a layered earth to an arbitrary source by using the fast Fourier transform (FFT). Starkhov [7] has given the convolution approach for evaluation of the Hankel transform integral. An entirely new approach—with application of a linear digital filter—for computation of the mutual coupling ratios on the surface of a multilayered earth for the horizontal coplanar, perpendicular, vertical coplanar, and vertical coaxial loop configurations has been developed by Koefoed *et al.* [8], Verma and Koefoed [9], and Verma [10] (displacement currents are neglected).

For the analysis in this paper, the linear digital filter method has been used with short filters and the variable cutoff notion (Verma and Koefoed [9]) for computing the mutual coupling ratios on the surface of a three-layer earth to study the detectability effect for the four EM sounding systems; the systems are compared for the relative effectiveness.

Computational Considerations

Classical Method

The classical method of computing the EM response of a layered earth involves evaluation of the infinite integrals giving the fields about a low-frequency oscillating magnetic dipole (Wait [3], Frischknecht [1]) by numerical integration on a digital computer.

Frischknecht [1] has presented extensive tables of mutual coupling ratios for horizontal coplanar, perpendicular, vertical coplanar, and vertical coaxial loop configurations on and above a two-layer ground by numerical integration of the following infinite integrals by the Gaussian quadrature method using a 16-point formula:

$$T_0(A,B) = \int_0^\infty R(D,g)\, g^2\, e^{-gA}\, J_0(gB)\, dg$$

$$T_1(A,B) = \int_0^\infty R(D,g)\, g^2\, e^{-gA}\, J_1(gB)\, dg$$

$$T_2(A,B) = \int_0^\infty R(D,g)\, g\, e^{-gA}\, J_1(gB)\, dg \qquad (1)$$

with

$$R(D,g) = 1 - 2g\,\frac{(U+V) + (U-V)\,e^{-UD}}{(U+g)(U+V) - (U-g)(U-V)\,e^{-UD}}$$

$$U = (g^2 + 2i)^{1/2}$$

$$V = (g^2 + 2ik)^{1/2}$$

Manuscript received March 19, 1977.

The author is with the National Geophysical Research Institute, Hyderabad, India.

$$k = \sigma_2/\sigma_1$$

$$\delta = (2/\omega\mu_0\sigma_1)^{1/2}$$

$$A = (z + h)/\delta$$

$$B = (r/\delta)$$

$$D = (2d/\delta)$$

where

ω	angular frequency;
δ	skin depth;
μ_0	magnetic permeability for free space;
h	height at which the oscillating magnetic dipole is located above a two-layer earth;
r	trasnmitter-receiver coil separation;
σ_2, σ_1	conductivities of the second and first layer, respectively;
d	thickness of the first layer;
J_0, J_1	Bessel functions of the first kind;
g	variable of integration.

The mutual coupling ratios for the four systems are given as

1) horizontal coplanar loops: $(Z/Z_0)_{\mathrm{I}} = 1 + B^3 T_0$;
2) perpendicular loops: $(Z/Z_0)_{\mathrm{II}} = B^3 T_1$;
3) vertical coplanar loops: $(Z/Z_0)_{\mathrm{III}} = 1 + B^2 T_2$;
4) vertical coaxial loops: $(Z/Z_0)_{\mathrm{IV}} = 1 + (0.5)\, B^2 (T_2 - BT_0)$.

(2)

($A = 0$, in integrals T_0, T_1, and T_2 when the loops are on the ground.)

Linear Digital Filter Method

Evaluation of the infinite integrals T_0, T_1, and T_2 in (1) by numerical integration is a time consuming task as the integrals contain products involving Bessel functions and these products are oscillatory.

The linear digital filter method (convolution method) (Koefoed *et al.* [8], Verma and Koefoed [9], Verma [10]) developed at the geophysical laboratory of the Delft University of Technology, Holland, is accurate and extremely fast in application relative to the numerical integration techniques. The central processing unit (CPU) time on an IBM 360/65 computer for the response for the horizontal coplanar loops system using short filter with variable cutoff (Verma and Koefoed [9]) over a three-layer earth model was found to be less than 0.3 s per value of the mutual coupling ratio. A brief review of the linear digital filter method as applied in computing the EM response of a multilayered earth is now in order.

The fundamental equations for the magnetic field generated by a vertical oscillating dipole located at the surface of a horizontally stratified earth have been given by Kozulin [11]. The following is the expression for the EM vector potential F generated in a point at or above the surface of the earth under conditions considered by Kozulin [11]:

$$F_z = C\left\{(1/r') + \int_0^\infty R(\lambda, d_i, \sigma_i, f)\, e^{-\lambda z} J_0(\lambda r)\, d\lambda\right\}. \quad (3)$$

The components of the vector potential in the horizontal plane are zero, and the radiation term in the Maxwell equation has been neglected.

The transmitting dipole is considered to be located at the origin of the cylindrical coordinate system with the z axis directed vertically upward. The point at which the vector potential has been considered has the coordinates r and z. In the expression (3) we have the following:

C	a constant;
d_i	thicknesses of the subsurface layers;
f	frequency;
J_0	Bessel function of order zero;
$R(\lambda)$	kernel function;
σ_i	conductivities of the subsurface layers;
r'	$= (r^2 + z^2)$;
λ	variable of integration.

The kernel function $R(\lambda)$ can be computed from the subsurface layer parameters and the frequency using a recurrence relation. Setting

$$R(\lambda) = R_{0,n}(\lambda)$$

in which the first suffix represents consideration of the field in space above the ground surface, and the second suffix n is the number of subsurface layers, the recurrence relation is the following (using the notation as used by Koefoed *et al.* [8]):

$$R_{(i-1),n}(\lambda) = \frac{V_{(i-1),i} + R_{i,n}(\lambda)\, e^{-2d_i V_i}}{1 + V_{(i-1),i} R_{i,n}(\lambda)\, e^{-2d_i V_i}} \quad (4)$$

and

$$R_{n,n}(\lambda) = 0$$

where

$$V_i = (\lambda^2 + \nu_i^2)^{1/2}$$
$$\nu_i^2 = j\,2\pi\mu_0\sigma_i f$$
$$V_{i,k} = (V_i - V_k)/(V_i + V_k).$$

The expressions for the components of the magnetic field strength can be obtained from (3). The relation between the magnetic field strength and the vector potential can be written as

$$\vec{H} = \text{grad div } \vec{F} - \nu^2 \vec{F} \quad (5)$$

and consideration of the field in the space above the ground surface implies that

$$\nu^2 = \nu_0^2 = j\,2\pi\mu_0\sigma_0 f = 0$$

reducing (5) to

$$\vec{H} = \text{grad div } \vec{F}. \quad (6)$$

Recalling that the components of F in the horizontal plane are zero, (6) under these conditions changes to

$$\vec{H} = \text{grad}\left(\frac{\partial}{\partial z} F_z\right)$$

or

$$H_z = \frac{\partial^2}{\partial z^2} F_z \quad (7)$$

and

$$H_r = \frac{\partial^2}{\partial z\, \partial r} F_z. \tag{8}$$

The expressions for the response function in terms of the mutual coupling ratio (Z/Z_0) can be obtained by first deriving the expressions for the components of the magnetic field strength with the help of (7), (8), and (3), and then dividing them by the free-space magnetic field strength term.

Applying the differentiations indicated in (7) and (8) to (3) and then setting $z = 0$, we have, for the components of the magnetic field strength at a point at the surface of the earth, the expressions

$$H_z = -\frac{C}{r^3} + C\int_0^\infty \lambda^2 R(\lambda, d_i, \sigma_i, f) J_0(\lambda r)\, d\lambda \tag{9}$$

$$H_r = C\int_0^\infty \lambda^2 R(\lambda, d_i, \sigma_i, f) J_1(\lambda r)\, d\lambda. \tag{10}$$

Dividing the right-hand side of (9) and (10) by the free-space term $(-C/r^3)$ gives, respectively, the response function for the horizontal coplanar loops system,

$$(Z/Z_0)_{\mathrm{I}} = 1 - \int_0^\infty r^3 \lambda^2 R(\lambda, d_i, \sigma_i, f) J_0(\lambda r)\, d\lambda \tag{11}$$

and the response function for the perpendicular loops system,

$$(Z/Z_0)_{\mathrm{II}} = -\int_0^\infty r^3 \lambda^2 R(\lambda, d_i, \sigma_i, f) J_1(\lambda r)\, d\lambda. \tag{12}$$

For the purpose of deriving the convolution integral, introducing new variables x and y as

$$\lambda = e^{-y} \qquad y = \ln(1/\lambda) \qquad d\lambda = -e^{-y}\, dy$$
$$r = e^x \qquad x = \ln(r) \tag{13}$$

(x and y define the logarithmic scales), (11) and (12) can be written as

$$(Z/Z_0)_{\mathrm{I}} = 1 - \int_{-\infty}^{+\infty} e^{3(x-y)} R(y, d_i, \sigma_i, f) J_0(e^{x-y})\, dy \tag{14}$$

$$(Z/Z_0)_{\mathrm{II}} = -\int_{-\infty}^{+\infty} e^{3(x-y)} R(y, d_i, \sigma_i, f) J_1(e^{x-y})\, dy. \tag{15}$$

It is seen that the integral in these equations is a convolution integral, and that the integral is a function of the layer parameters, the frequency, and x. It follows that the relation between the integral as a function of x and the EM kernel function as a function of y (for given values of frequency and the layer parameters) is a linear relation.

The integrals in (14) and (15) are convolutions of two functions. One of these can be taken as the filter function, the other as the input function to the filter. Consideration of the part of the integrand to be taken as the filter function needs special care for the reason that all the choices would not be equally good for practical application in that for some of them the integral may not converge to zero for both large positive and large negative values of x; for others, the convergence to zero on both sides may be too slow and thus contain a large number of digital filter coefficients. For these reasons the criterion of "fast convergence" is used in making the choice of the filter function.

The following optimum choices were made for the horizontal coplanar and perpendicular loops systems in computing the response functions derived in (14) and (15):

horizontal coplanar loops system:

$$\text{input function} = -e^{2(x-y)} R(y, d_i, \sigma_i, f)$$
$$\text{filter function} = e^{(x-y)} J_0(e^{x-y}) \tag{16}$$

perpendicular loops system:

$$\text{input function} = -e^{2(x-y)} R(y, d_i, \sigma_i, f)$$
$$\text{filter function} = e^{(x-y)} J_1(e^{x-y}). \tag{17}$$

For the vertical coplanar loops system, the filter function is the same as that for the perpendicular loops system given in (17), but the input function is in the modified form:

$$\text{input function} = -e^{(x-y)} R(y, d_i, \sigma_i, f). \tag{18}$$

For deriving the digital filter, the input function was approximated as a sum of sinc functions. The integrals in (14) and (15) are the output functions corresponding to input and filter functions defined in (16) and (17). Obviously, the output function is then a sum of integrals in which the integrand is the product of a sinc function with the filter function; the integral for unit amplitude of the sinc function is referred to as the sinc response of the filter. The evaluation of the sinc response of the filter is determined by operating on the spectra of the functions in the following manner:

1) selection of suitable input and output functions;
2) determination of the Fourier transforms of both the input and output functions;
3) the filter spectrum is then the quotient of the spectrum of the output function over the spectrum of the input function;
4) multiplication of the filter spectrum by the spectrum of the sinc function, resulting in the spectrum of the sinc response which is cutoff at the Nyquist frequency;
5) taking the inverse Fourier transform of the spectrum of the sinc response gives the desired sinc response of the filter (i.e., filter weights).

(A sampling interval of ln 10/10 was found adequate to reconstruct the actual input function between the sample points with an absolute error of less than 10^{-5}.)

The length of the digital filter that is required to obtain a prescribed accuracy in computing the mutual coupling ratio has been determined by studying the values of the digital filter coefficients in conjunction with the range of values which the input functions may assume (Verma and Koefoed [9]). It has been found that the required filter length (for short filters)

depends on the ground layer parameters, the loop spacing, and the frequency. This dependence resulted in application of the "variable cutoff notion" and the empirical equations involving variable cutoff for the digital filters for the EM sounding response functions determined. These are given as follows.

For the horizontal coplanar loops system,

$$KS = \text{ENTIER } \{4 \ln (1000\, d_1/r)\} \tag{19}$$

where

d_1 thickness of the first layer;
r transmitter-receiver coil separation;
ENTIER (E) transfer function for an expression of the real type, E, which "transfers" E to one of the integer type, and assigns to it the value which is largest integer not greater than the value of E;
KS subscript for the first filter coefficient that needs to be used (upper limit for KS is 22).

For the perpendicular loops system,

$$KS = \text{ENTIER } 2.5\ \{\ln (10^9\ \rho T/r^2)\} \tag{20}$$

where

ρ smallest resistivity that occurs in the layer sequence;
T period (1/frequency);
r transmitter-receiver coil separation;
KS subscript for the first filter coefficient that needs to be used (upper limit for KS is 17).

For the vertical coplanar loops system,

$$KS = \text{ENTIER } \{1.3 \ln (10^9\ \rho T/r^2)\} \tag{21}$$

where

ρ smallest resistivity that occurs in the layer sequence;
KS subscript for the first filter coefficient that needs to be used (upper limit for KS is 11).

The manner in which the filter coefficients and their abscissas are applied to the convolution sum, along with the filter weights for the different EM systems, is given in the Appendix.

It should be remarked that the linear digital filter method as developed by Koefoed *et al.* [8] and Verma and Koefoed [9] has gained wide application in computation of a class of convolution integrals, and a great deal of work in this line has been reported as being currently pursued at the U.S. Geological Survey, Denver (Anderson [12]-[15]).

Detectability of Subsurface Layers

The multilayer computer program using "short filters with variable cutoff" has been used to study the detectability effect of subsurface layers by the four EM systems: horizontal coplanar loops, perpendicular loops, vertical coplanar loops, and vertical coaxial loops. Although phase data in some cases give a better resolution compared to real, imaginary, and modulus plots, we have used $|Z/Z_0|$ for the response function all along.

For the multifrequency EM sounding plots, the parameter T (period) instead of frequency has been plotted on a logarithmic scale along the abscissa and $|Z/Z_0|$ along the ordinate on linear scale. The frequency sounding plots are in 30 points; frequency varied in the range 1-100 000 Hz.

The following subsurface layering situations (three-layer cases) have been analyzed with the indicated range of parameters.

1) For an intermediate conductive layer

$\rho_2/\rho_1 = 1/20 \quad \rho_3/\rho_1 = 1$

$d_2/d_1 = 1/4,\ 1/20 \quad d_1/r = 0.067$ to 2.

2) For an intermediate resistive layer,

$\rho_2/\rho_1 = 20 \quad \rho_3/\rho_1 = 1$

$d_2/d_1 = 1/4,\ 1/20 \quad d_1/r = 0.067$ to 2.

3) For a descending-type resistivity distribution,

$\rho_2/\rho_1 = 0.316 \quad \rho_3/\rho_2 = 0.316$

$d_2/d_1 = 1 \quad d_1/r = 0.02$ to 1.

4) For an ascending-type resistivity distribution,

$\rho_2/\rho_1 = 3.16 \quad \rho_3/\rho_2 = 3.16$

$d_2/d_1 = 2 \quad d_1/r = 0.02$ to 1.

For computing the "detectability effect," the variation of the modulus of the mutual coupling ratio (Z/Z_0) with frequency was first calculated. Next, $|Z/Z_0|$ values were computed for the homogeneous earth model for the intermediate conductive and resistive layer cases, respectively, and the two-layer earth model for the descending- and ascending-type cases, respectively. The difference between these two sets of values computed at each value of the frequency then represents the effect due to the presence of the sandwiched layer in the three-layer earth section. For the analyses, the percentile difference between the two sets of values at each frequency has been used; although in the figures the variation of $|Z/Z_0|$ with T(1/frequency) is presented, as it shows clearly the range of frequencies in which the hidden layer is detectable. The percentile difference, as an example, has been shown in Fig. 13 for the horizontal coplanar loops system in the Appendix.

Intermediate Conductive Layer

The EM response curves have been computed with the following numerical values for the layer parameters and the coil spacings:

$\rho_1 = 1000\ \Omega \cdot \text{m} \quad \rho_2 = 50\ \Omega \cdot \text{m} \quad \rho_3 = 1000\ \Omega \cdot \text{m}$

$d_1 = 200$ m $\quad d_2 = 10$ m and 50 m $\quad r = 100$-3000 m.

The three-layer curves have been compared with the homogeneous earth curve when the medium is considered to be homogeneous with a resistivity the same as that of the top layer ($1000\ \Omega \cdot \text{m}$). In the figures, the three-layer curve has been shown in solid lines; the dotted line represents the homogeneous earth curve. Although the computations have been made for a large range of loop separations, only a few have been included for the sake of brevity.

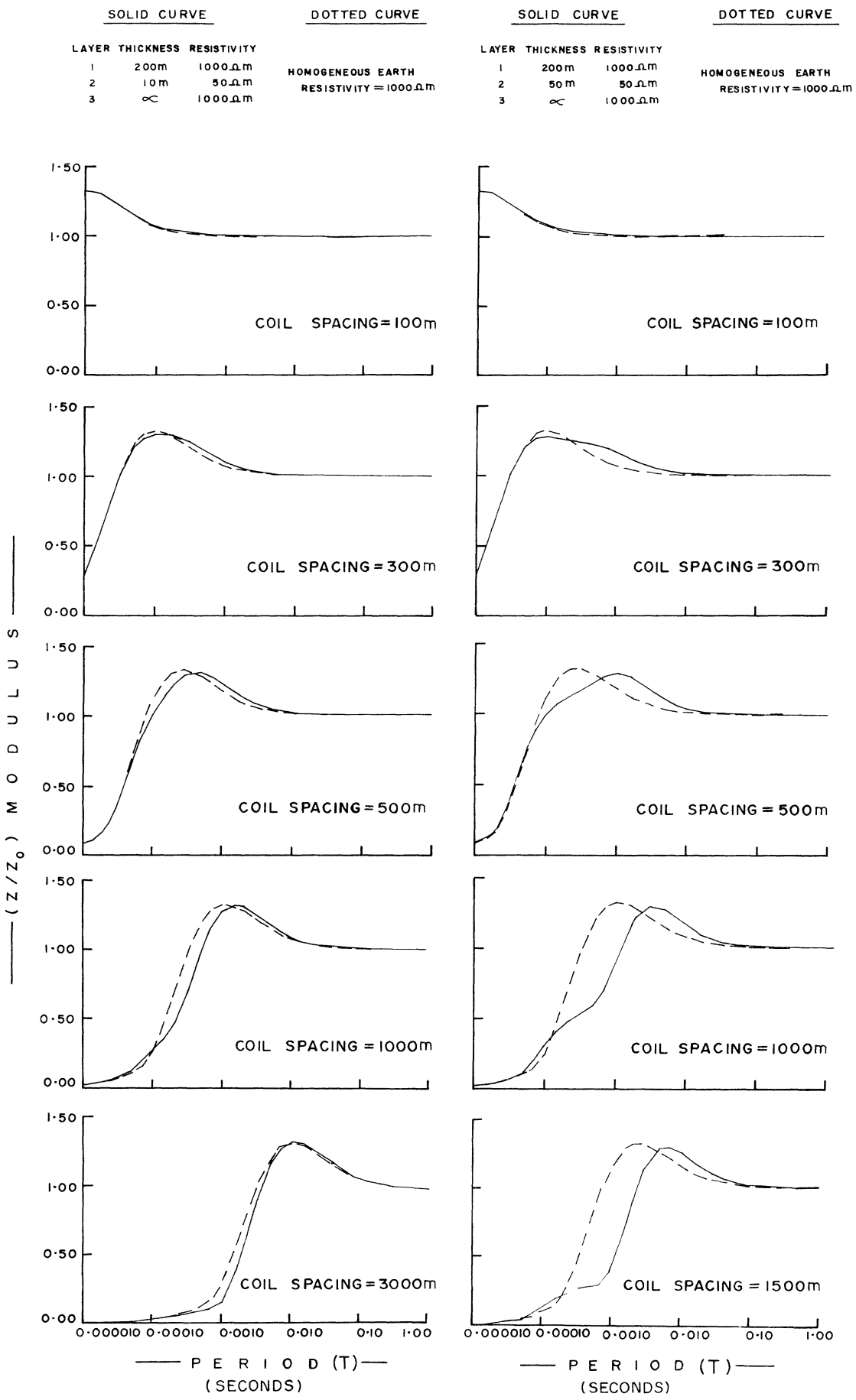

Fig. 1. Plot of $|Z/Z_0|$ versus period T(1/frequency) for the intermediate conductive layer for two values of the layer thickness ratio 1/20 and 1/4 for the horizontal coplanar loops system.

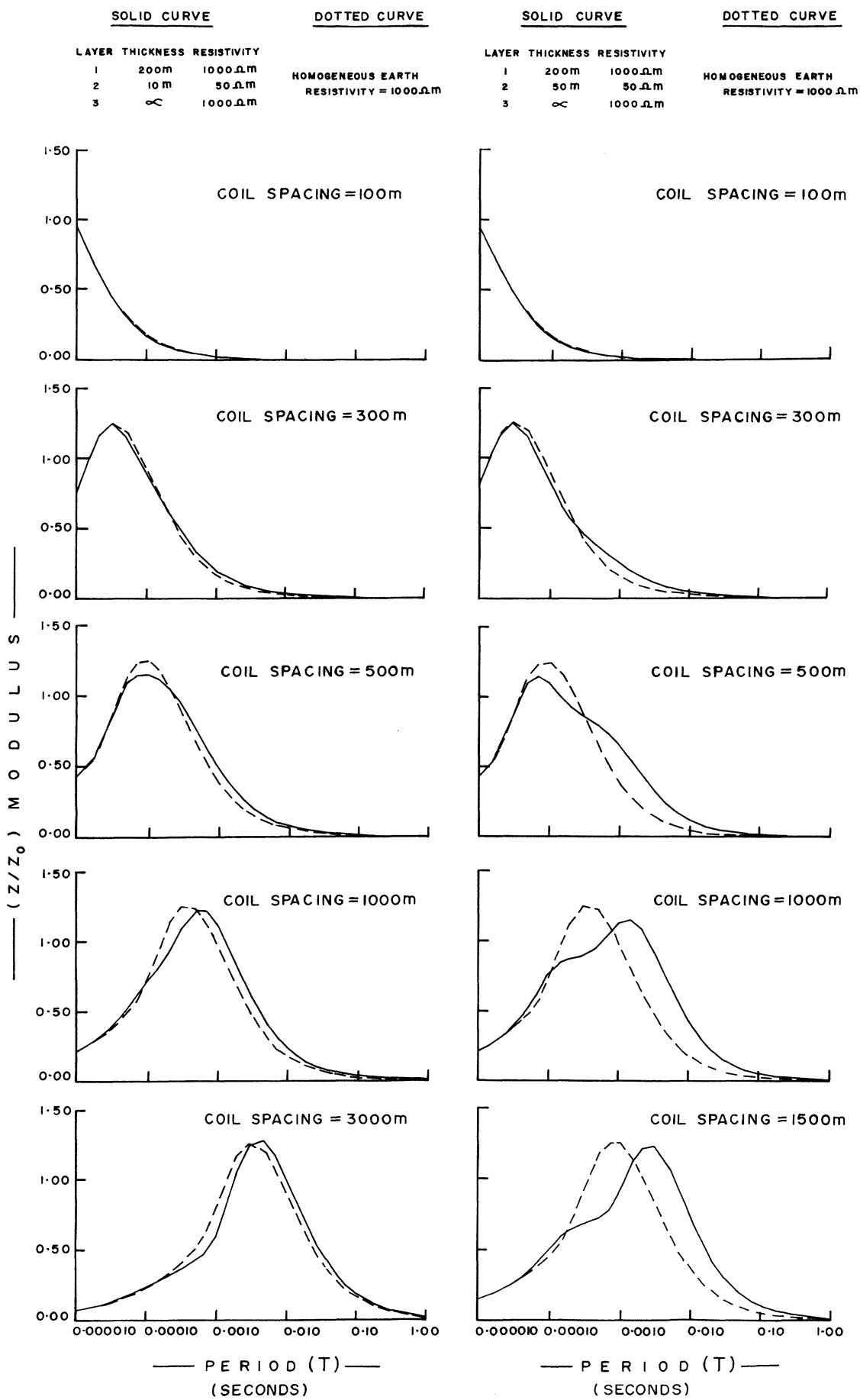

Fig. 2. Plot of $|Z/Z_0|$ versus period T(1/frequency) for the intermediate conductive layer for two values of the layer thickness ratio 1/20 and 1/4 for the perpendicular loops system.

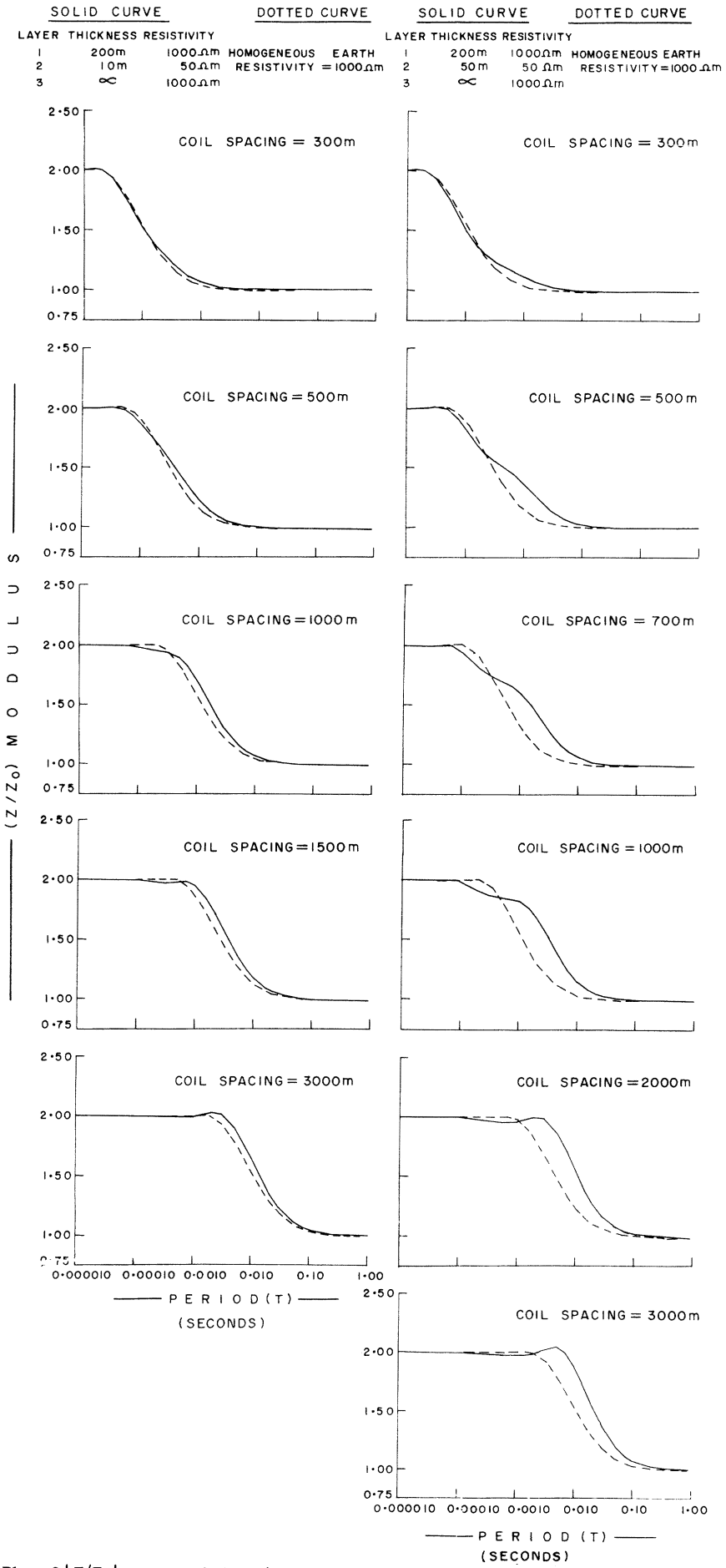

Fig. 3. Plot of $|Z/Z_0|$ versus period T(1/frequency) for the intermediate conductive layer for two values of the layer thickness ratio 1/20 and 1/4 for the vertical coplanar loops system.

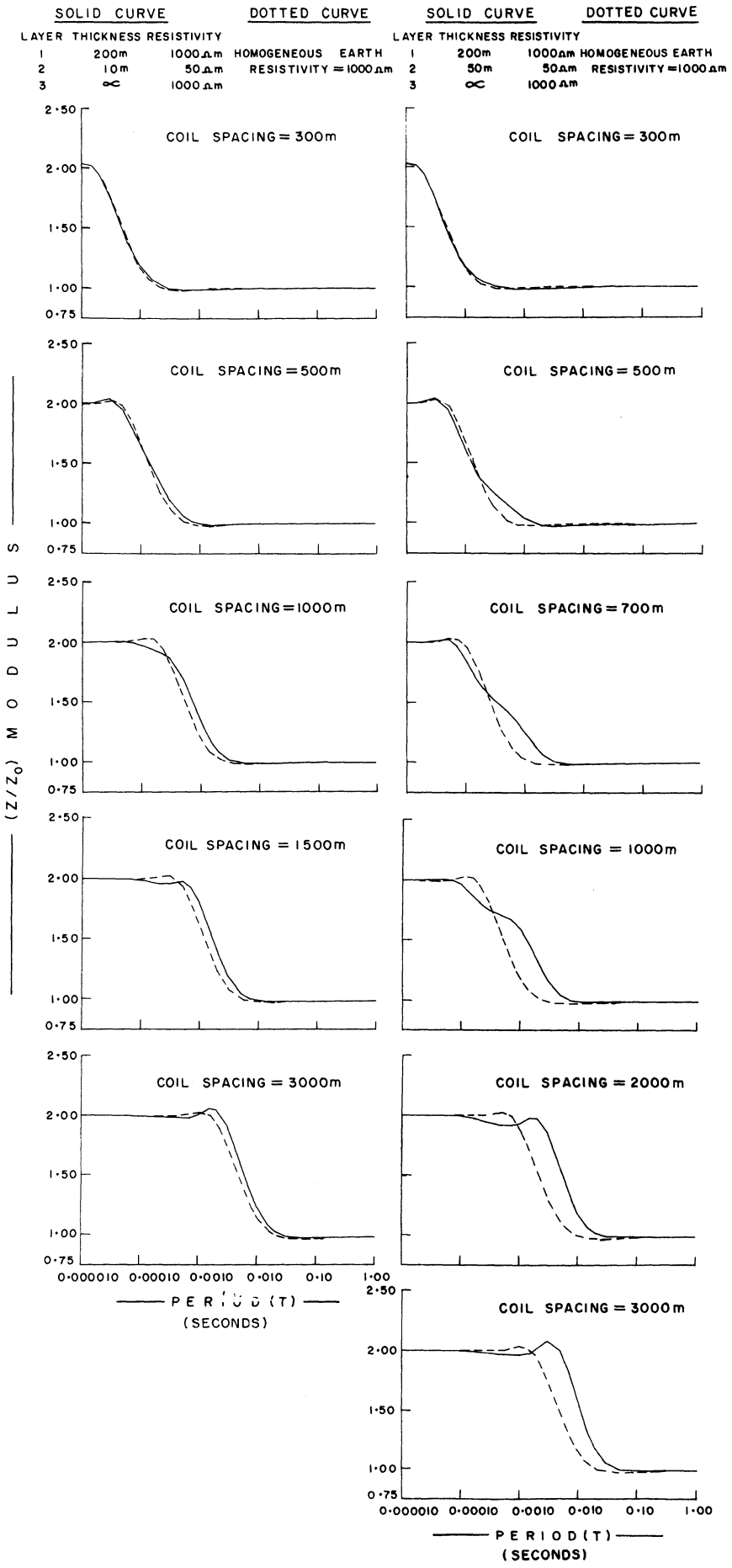

Fig. 4. Plot of $|Z/Z_0|$ versus period T(1/frequency) for the intermediate conductive layer for two values of the layer thickness ratio 1/20 and 1/4 for the vertical coaxial loops system.

Horizontal Coplanar Loops Systems: $d_2/d_1 : 1/20$–It should be stressed that the resolution of the frequency sounding depends upon the degree of dissimilarity in shape between the response curves for different parameters. For this ratio of the layer thickness, the strength of the "detectability effect" (this will be referred as "effect" all along) is generally appreciable for detection of the thin interbedded layer (10 m thick) (Fig. 1). It is seen that the effect enhances with increase in the coil spacings (i.e., decrease in the ratio: d_1/r) and subsequently attains the saturation value around $r = 1000$ m.

$d_2/d_1 : 1/4$–In this case the overall effect is relatively stronger (Fig. 1). It is thus obvious that the detectability would be better with increase in the d_2/d_1 ratio, as expected. The saturation values are reached between $r = 700$ m and $r = 1000$ m.

Perpendicular Loops System: $d_2/d_1 : 1/20$–For this layer thickness ratio the trend of the effect is similar to that in the horizontal coplanar loops system; the saturation value is reached around $r = 1000$ m (Fig. 2).

$d_2/d_1 : 1/4$–The strength of the effect, all along, is about the same as in the horizontal coplanar loops system for this ratio of the layer thickness (Fig. 2). The saturation value is around $r = 1000$ m.

Comparing the horizontal coplanar and perpendicular loops systems, it is seen that the range of frequencies in which the hidden layer is detectable is about the same in both systems. This implies that on the descending part of the response curve the relative change in $|Z/Z_0|$ is larger for the perpendicular loops system than for the horizontal coplanar loops system. Thus for a particular type of application, depending upon the performance of the instrument available, and existing geological conditions either of the two systems could be used.

Vertical Coplanar Loops System: $d_2/d_1 : 1/20$–The effect generally appears to be reasonably strong (Fig. 3). It is appreciable at $r = 500$ m and attains the saturation value around $r = 1000$ m.

$d_2/d_1 : 1/4$–As compared to the previous case, the effect for this ratio of the layer thickness is stronger. Again, this is to be attributed to the increase in the layer thickness ratio (Fig. 3). Saturation is reached around $r = 1000$ m.

Vertical Coaxial Loops System: $d_2/d_1 : 1/20$–The effect is quite comparable, though a bit inferior, to that in the vertical coplanar loops system. Saturation is attained around $r = 1000$ m (Fig. 4).

$d_2/d_1 : 1/4$–As would be expected, the overall effect is much stronger for this case with a higher layer thickness ratio (Fig. 4). The saturation value is reached around $r = 1000$ m.

When vertical coplanar loops and vertical coaxial loops systems are compared, although the overall effect is comparable, it is relatively weaker in the coaxial loops system for lower coil separations. It may be remarked that as the shape of the EM response curve for both systems is about the same (with reference to the magnitude), the relative change in effect, when both the systems are compared, is not very appreciable.

In brief, it may be concluded that for the detection of the intermediate conducting layer, the perpendicular loops system appears to be superior to the horizontal coplanar loops system; the effects in the vertical coplanar loops and vertical coaxial loops systems are comparable among themselves, but weaker than in the horizontal coplanar loops system.

Intermediate Resistive Layer

The numerical values used for the layer parameters and loop spacings are the following:

$\rho_1 = 50\ \Omega \cdot m$ $\quad \rho_2 = 1000\ \Omega \cdot m$ $\quad \rho_3 = 50\ \Omega \cdot m$

$d_1 = 200$ m $\quad d_2 = 10$ m and 50 m $\quad r = 100$–3000 m.

The three-layer curves have been compared with the homogeneous earth curve when the medium is considered to be homogeneous with a resistivity the same as that of the top layer ($50\ \Omega \cdot m$).

Horizontal Coplanar Loops System: $d_2/d_1 : 1/20$–The effect in general is very weak (Fig. 5).

$d_2/d_1 : 1/4$–As compared to the previous case, the effect seems to be relatively improved for this value of the layer thickness ratio, although weak in general (Fig. 5).

Perpendicular Loops System: $d_2/d_1 : 1/20$–As in the horizontal coplanar loops system, the overall effect for this system is also very weak throughout (Fig. 6).

$d_2/d_1 : 1/4$–The effect in this system is comparable to that in the horizontal coplanar loops system for this ratio of the layer thickness (Fig. 6).

It is thus seen that the effect in both systems is weak for the purpose of detection of the intermediate resistive layer.

Vertical Coplanar Loops System: $d_2/d_1 : 1/20$–The strength of the effect throughout is weak (Fig. 7).

$d_2/d_1 : 1/4$–The effect is stronger compared to that for the previous case possibly to the degree that it could marginally be used for the detection of the intermediate resistive layer (Fig. 7).

Vertical Coaxial Loops System: $d_2/d_1 : 1/20$–The effect in general is weak and this system has a behavior similar to that of the vertical coplanar loops system (Fig. 8).

$d_2/d_1 : 1/4$–The overall effect is stronger in this case and its behavior is similar to that for the vertical coplanar loops system (Fig. 8).

Comparing the effects in vertical coplanar loops and vertical coaxial loops systems, although the strength in both systems is comparable, they are weak. However, for coil separations lower than 1000 m, the effect in the vertical coaxial loops system appears to be relatively better.

It may be concluded that the response of the four EM sounding systems for the detection of the intermediate resistive layer is in general poor.

Descending-Type Resistivity Distribution

For the descending-type three-layer case, for the computations, the following numerical values have been used for the layer parameters and the loop separations:

$\rho_1 = 1000\ \Omega \cdot m$ $\quad \rho_2 = 1000/\sqrt{10}\ \Omega \cdot m$ $\quad \rho_3 = 100\ \Omega \cdot m$

$d_1 = 100$ m $\quad d_2 = 100$ m $\quad r = 100$–5000 m.

For the "detectability effect," the descending-type three-layer curve (solid line in figures) has been compared with the two-layer curve (dotted line in figures). For computing the two-layer curve, out of the parameters for the descending-type three-layer curve, d_1 has been chosen such as to approach the three-layer curve (with descending resistivity distribution).

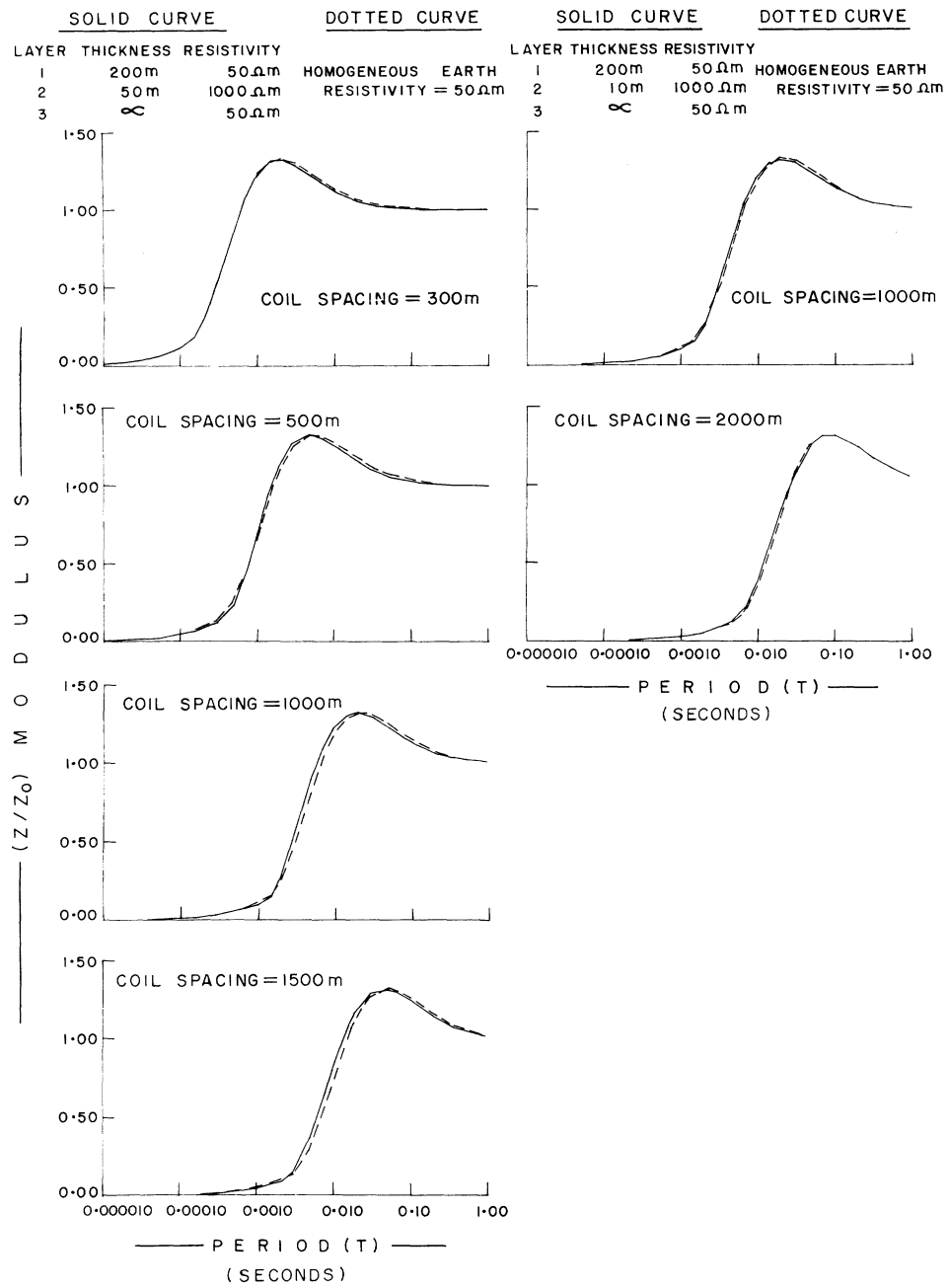

Fig. 5. Plot of $|Z/Z_0|$ versus period T(1/frequency) for the intermediate resistive layer for two values of the layer thickness ratio 1/20 and 1/4 for the horizontal coplanar loops system.

The following numerical values have been used to compute the two-layer curve:

$\rho_1 = 1000\ \Omega \cdot \text{m}$ $\rho_2 = 100\ \Omega \cdot \text{m}$

$d_1 = 172.5\ \text{m}$ $r = 100\text{-}5000\ \text{m}$.

Horizontal Coplanar Loops System: The overall strength of the effect may be rated as good from the point of view of the detectability (Fig. 9). The effect is apparent at lower coil separations and attains the maximum value between $r = 500$ m and $r = 700$ m, then falls off gradually to the extent that it is hardly noticeable at a coil separation of 5000 m.

Perpendicular Loops System: The overall strength of the effect and its variation with increase in the coil separation is similar to that for the horizontal coplanar loops system (Fig. 9). The maximum in effect occurs between $r = 500$ m and $r = 1000$ m, then reduces gradually with increase in the coil separations.

When the horizontal coplanar loops and perpendicular loops systems are compared for detectability, in both systems the degree of the effect is good. The relative change seems to be larger for the horizontal coplanar loops system than for the perpendicular loops system. However, for the perpendicular loops system, the range of the effect (as it is also apparent along the descending part of the response curve) is larger than for the horizontal coplanar loops system.

In general, either of the two systems could be effectively used for the detection of the descending-type layering situation.

Vertical Coplanar Loops System: The effect is reasonably good (Fig. 10). It shows up at smaller coil separations and attains a maximum value around $r = 500$ m, then reduces with

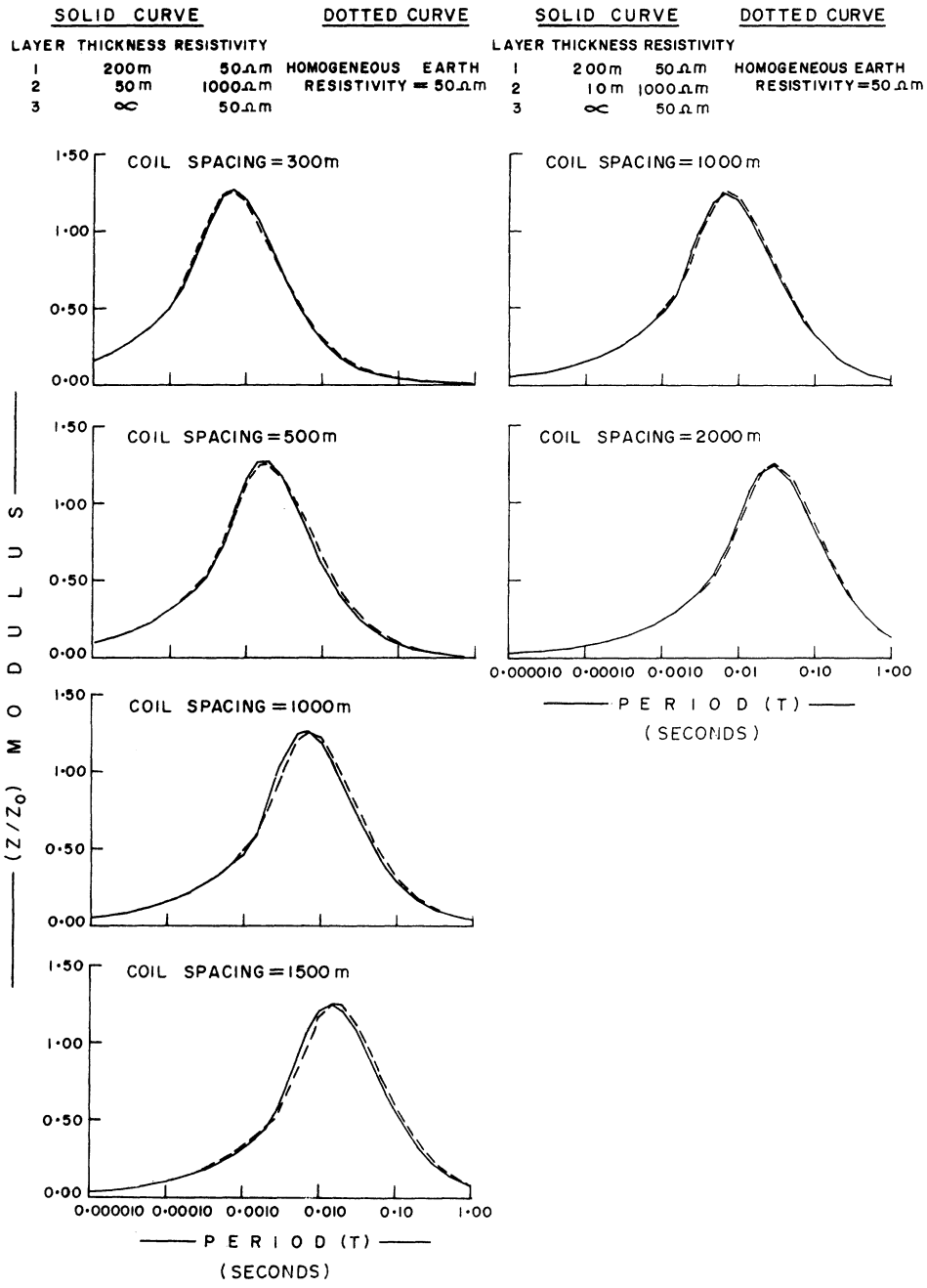

Fig. 6. Plot of $|Z/Z_0|$ versus period T(1/frequency) for the intermediate resistive layer for two values of the layer thickness ratio 1/20 and 1/4 for the perpendicular loops system.

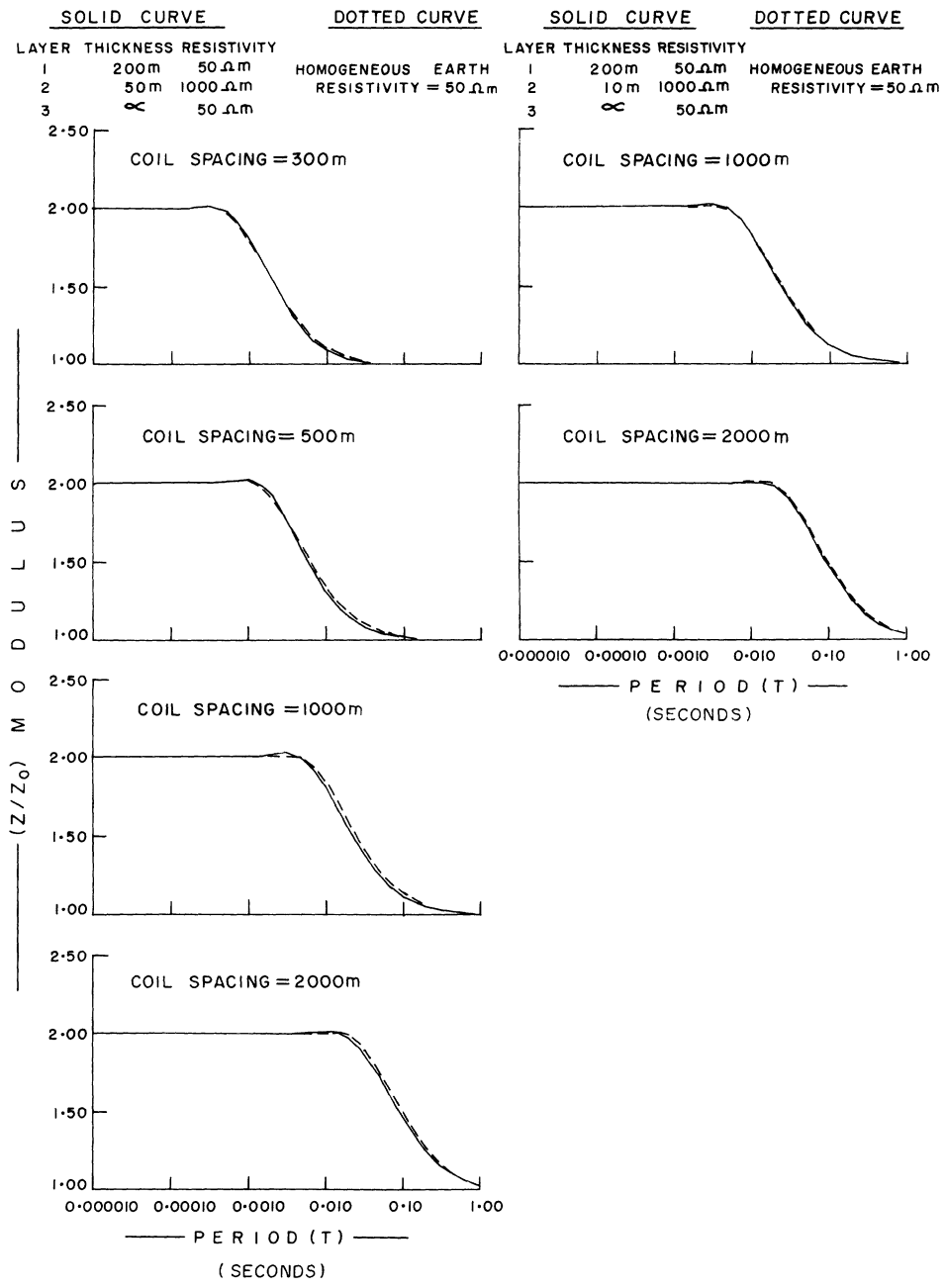

Fig. 7. Plot of $|Z/Z_0|$ versus period T(1/frequency) for the intermediate resistive layer for two values of the layer thickness ratio 1/20 and 1/4 for the vertical coplanar loops system.

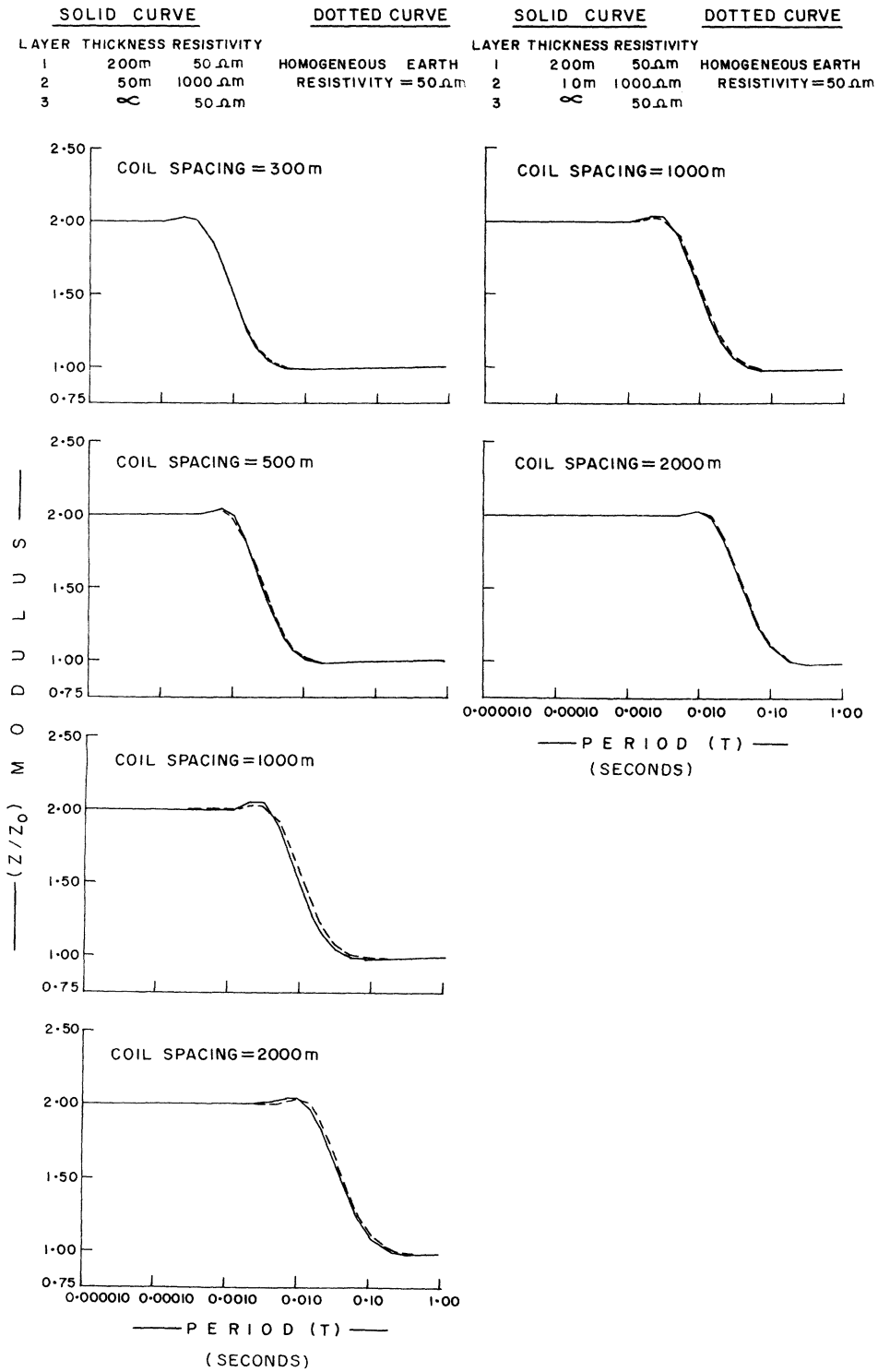

Fig. 8. Plot of $|Z/Z_0|$ versus period T(1/frequency) for the intermediate resistive layer for two values of the layer thickness ratio 1/20 and 1/4 for the vertical coaxial loops system.

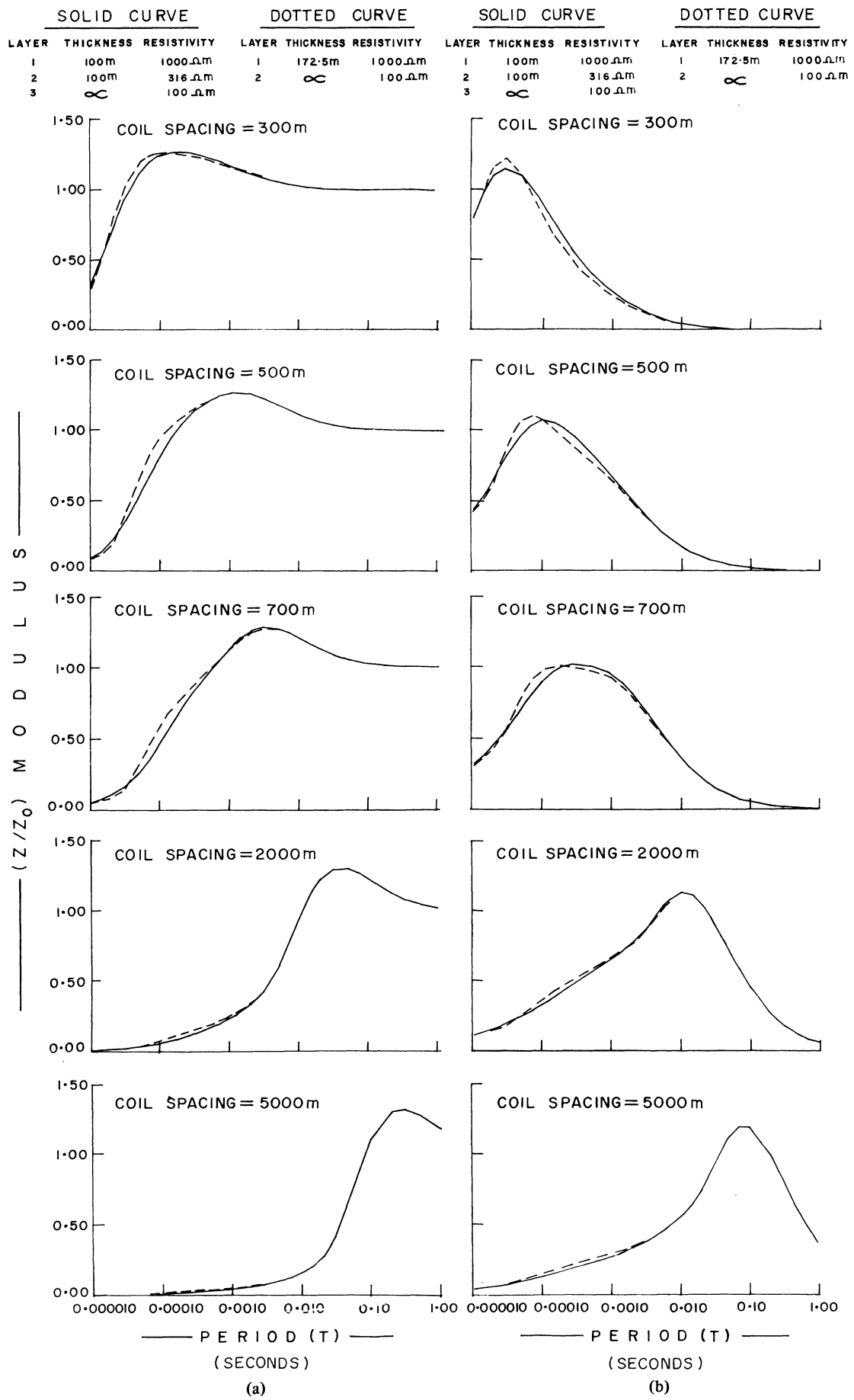

Fig. 9. Plot of $|Z/Z_0|$ versus period T(1/frequency) for the descending-type three-layer case for the (a) horizontal coplanar loops and (b) perpendicular loops systems.

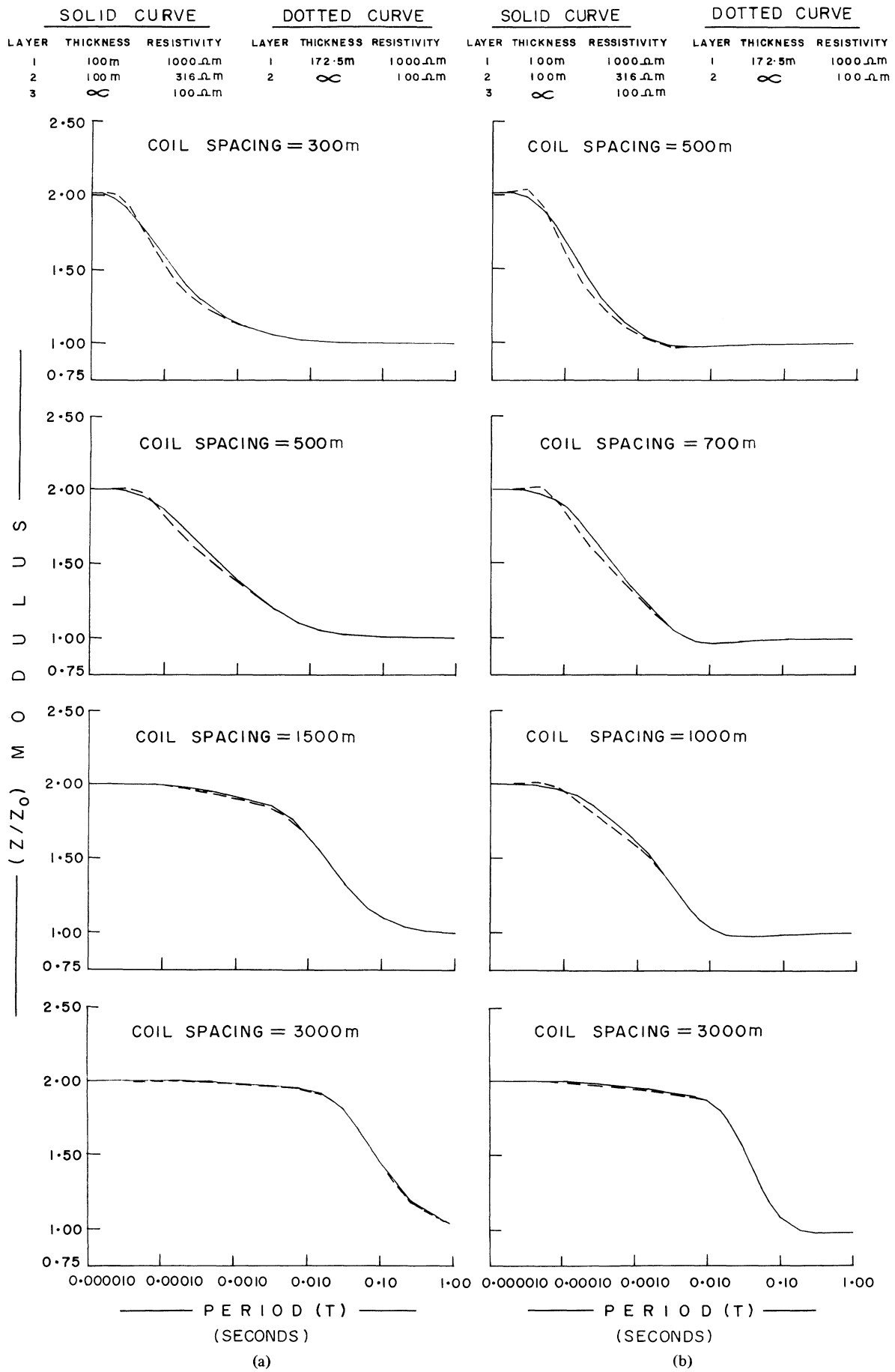

Fig. 10. Plot of $|Z/Z_0|$ versus period T(1/frequency) for the descending-type three-layer case for the (a) vertical coplanar loops and (b) vertical coaxial loops systems.

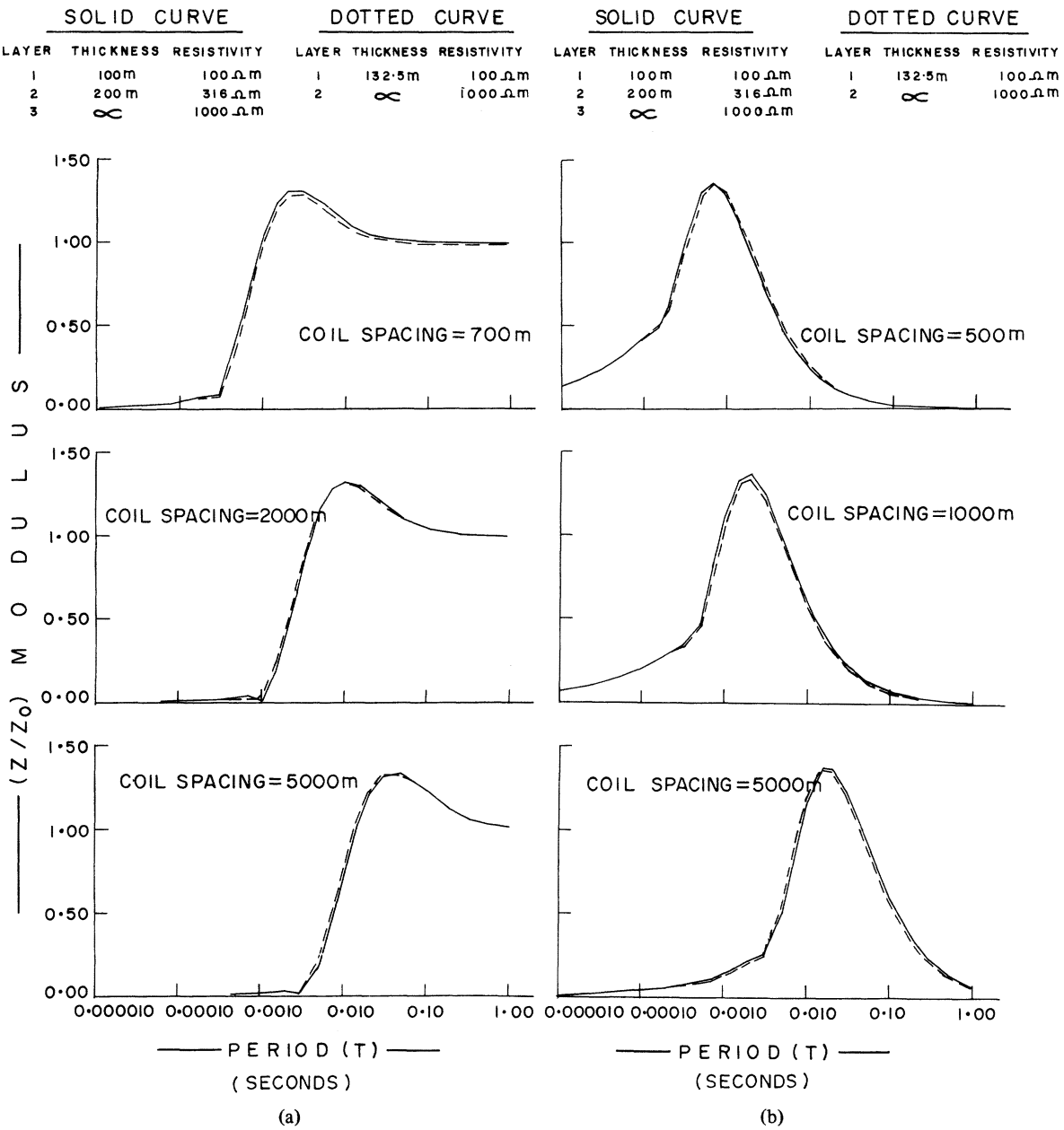

Fig. 11. Plot of $|Z/Z_0|$ versus period T(1/frequency) for the ascending-type three-layer case for the (a) horizontal coplanar loops and (b) perpendicular loops systems.

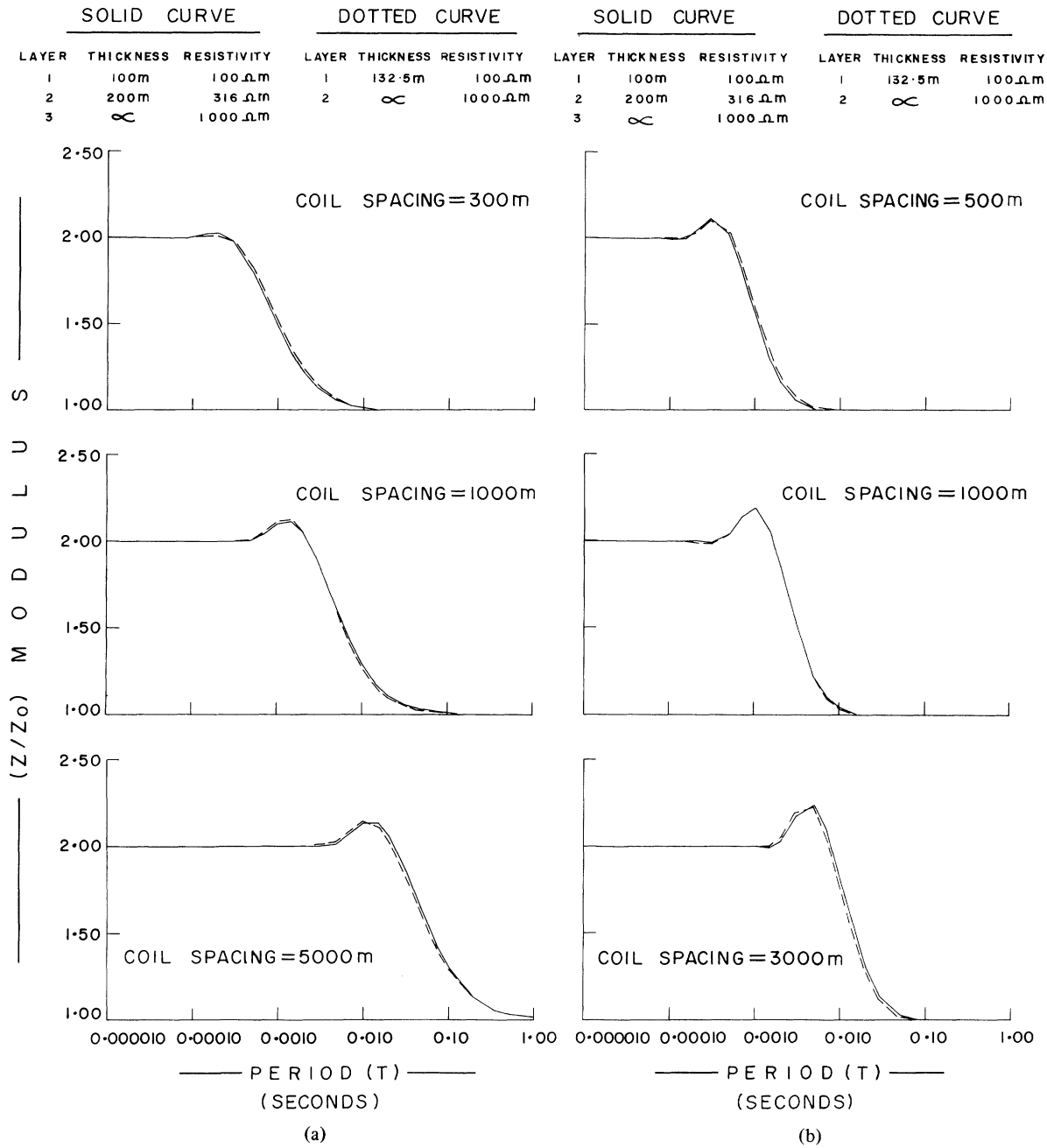

Fig. 12. Plot of $|Z/Z_0|$ versus period T(1/frequency) for the ascending-type three-layer case for the (a) vertical coplanar loops and (b) vertical coaxial loops systems.

increase in the coil separations. At $r = 3000$ m, the effect is hardly noticeable.

Vertical Coaxial Loops System: In general the strength of the effect and its nature of variation with increase in the coil separations is similar to that for the vertical coplanar loops system (Fig. 10). The maximum is at $r = 500$ m, and falls off afterwards.

When the two systems are compared, the effect in both systems is reasonably good and comparable. However, because of the relatively steeper nature of the response curve for the vertical coaxial loops system, the relative change in effect seems to be larger than for the vertical coplanar loops system.

Comparing all four EM sounding systems for the detectability effect, the effects in the horizontal coplanar loops and perpendicular loops systems are not appreciably different and thus they are comparable in general. However, the perpendicular loops system appears to be somewhat superior to the horizontal coplanar loops system in that the effect also shows up along the descending part of the response curve (corresponding to higher periods along abscissa) for a range of coil separations. In the vertical coplanar loops and vertical coaxial loops systems the effects are also generally comparable among themselves but weaker than in the horizontal coplanar loops and perpendicular loops systems. Yet the overall effect can be rated as fairly good for the detection of the subsurface layers having a descending-type resistivity distribution.

All in all, it may be concluded that depending upon the performance of the instrument used and existing geological conditions, any of the four systems could be effectively used for detecting such a layered situation.

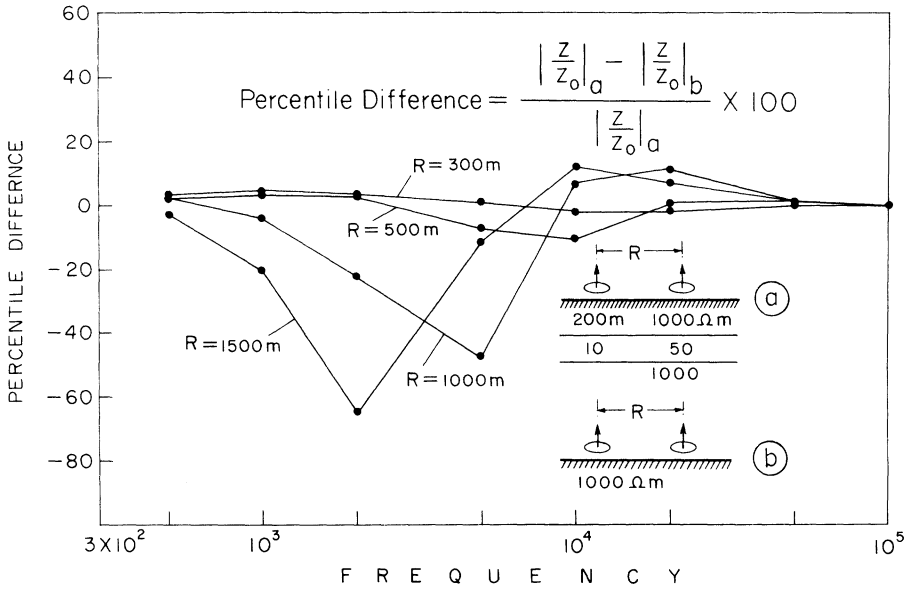

Fig. 13. Detectability effect of a conducting thin middle layer.

Ascending-Type Resistivity Distribution

For the ascending-type three-layer case, the following numerical values have been used for the layer parameters and coil separations:

$\rho_1 = 100\ \Omega \cdot m$ $\rho_2 = 100\sqrt{10}\ \Omega \cdot m$ $\rho_3 = 1000\ \Omega \cdot m$

$d_1 = 100$ m $d_2 = 200$ m $r = 100$–5000 m.

To study the detectability effect involved, the three-layer curve (solid line in figures) has been compared with the two-layer curve (dotted line in figures). The two-layer curve has been computed with an appropriate value for d_1 such that it approaches the three-layer ascending-type curve. Numerical values for the parameters used are as follows:

$\rho_1 = 100\ \Omega \cdot m$ $\rho_2 = 1000\ \Omega \cdot m$

$d_1 = 132.5$ m $r = 100$–5000 m.

Horizontal Coplanar Loops System: The strength of the effect in general is weak (Fig. 11). The maximum in effect is apparent at $r = 700$ m, which then reduces first and subsequently gains in strength approaching the saturation value.

Perpendicular Loops System: In this system also the overall effect is weak. The maximum value is attained around $r = 1000$ m (Fig. 11). Around $r = 1500$ m the strength reduces a little and then approaches the saturation value.

In general the strength of the detectability effect in both systems is weak. While the range of frequencies in both systems in which the sandwiched layer is detectable is about the same, the relative change in $|Z/Z_0|$ is larger for the perpendicular loops system along the descending part of the response curve then it is for the horizontal coplanar loops system.

Vertical Coplanar Loops System: The overall effect is weak and comparable to that for the horizontal coplanar loops and perpendicular loops systems. The maximum is reached at $r = 300$ m (Fig. 12), which first reduces and subsequently builds up after $r = 1000$ m approaching the saturation value.

Vertical Coaxial Loops System: The effect is comparable with that for the vertical coplanar loops system. The maximum is reached around $r = 500$ m (Fig. 12) and the saturation value at $r = 1000$ m. It is seen that the effect has considerably reduced at higher coil separations.

Comparing these two systems, the strength of the effect in both is weak, though comparable. Although the frequency range of the effect is about the same for both, the relative change is larger for the vertical coaxial loops system than for the vertical coplanar loops system.

Comparing the four systems considered, it may be concluded that the overall effect in all the systems is weak in general. The frequency range of the effect for all the systems is about the same, which implies that, based on the degree of steepness along the descending part of the EM response curves, the perpendicular loops system appears to be a bit superior to the horizontal coplanar loops system; the vertical coaxial loops system superior to the vertical coplanar loops system. However, as the degree of superiority involved is not very appreciable, all four systems could be rated as equally effective generally for the detection of ascending-type three-layer cases.

Appendix

The digital filter coefficients are applied in the following manner to the convolution sum:

$$\sum_{k=0}^{n} C_k \cdot f(Y_k)$$

where

C_k filter coefficient at abscissa values η_k;
$f(Y)$ input function;
Y_k $= X - \eta_k = \ln r - \eta_k = \ln r - \eta_0 + k \ln 10/10$
n suffix of the last filter coefficient that is used.

In Tables I-III are listed the filter weights for the horizontal coplanar loops, perpendicular loops, and vertical coplanar loops systems, respectively.

TABLE I
THE FILTER COEFFICIENTS AND THEIR ABSCISSA VALUES FOR HORIZONTAL COPLANAR LOOPS

K	η_K	C_k	K	η_k	C_k
0	+ 8.75198087	− .00001787	25	+ 2.99551814	+ .04821827
1	+ 8.52172236	+ .00000935	26	+ 2.76525963	− .13070863
2	+ 8.29146385	+ .00000375	27	+ 2.53500112	+ .31328618
3	+ 8.06120534	− .00001754	28	+ 2.30474261	− .51302191
4	+ 7.83094683	+ .00001084	29	+ 2.07448410	+ .31003396
5	+ 7.60068832	− .00000942	30	+ 1.84422559	+ .34216522
6	+ 7.37042981	+ .00000456	31	+ 1.61396708	− .20142642
7	+ 7.14017130	+ .00000394	32	+ 1.38370857	− .36288158
8	+ 6.90991280	− .00001576	33	+ 1.15345006	− .22914055
9	+ 6.67965429	+ .00003025	34	+ .92319155	− .03202792
10	+ 6.44939579	− .00004683	35	+ .69293304	+ .10252302
11	+ 6.21913727	+ .00006539	36	+ .46267454	+ .16941035
12	+ 5.98887876	− .00008669	37	+ .23241603	+ .18559086
13	+ 5.75862025	+ .00011278	38	+ .00215752	+ .17656063
14	+ 5.52836174	− .00014748	39	− .22810099	+ .15523408
15	+ 5.29810323	+ .00019692	40	− .45835950	+ .13149777
16	+ 5.06784472	− .00027055	41	− .68861801	+ .10841834
17	+ 4.83758621	+ .00038337	42	− .91887652	+ .08826593
18	+ 4.60732770	− .00056557	43	− 1.14913503	+ .07109834
19	+ 4.37706919	+ .00085297	44	− 1.37939354	+ .05708674
20	+ 4.14681068	− .00134318	45	− 1.60965205	+ .04555925
21	+ 3.91655217	+ .00224120	46	− 1.83991056	+ .03635105
22	+ 3.68629367	− .00404751	47	− 2.07016907	+ .02892500
23	+ 3.45603516	+ .00812962	48	− 2.30042758	+ .02289634
24	+ 3.22577665	− .01859531	49	− 2.53068609	+ .01843169
			50	− 2.76094460	+ .01454755

TABLE II
THE FILTER COEFFICIENTS AND THEIR ABSCISSA VALUES FOR PERPENDICULAR LOOPS

K	η_k	C_k	k	η_k	C_k
0	+ 7.48268832	+ .00001662	20	+ 2.87751814	− .08103193
1	+ 7.25242981	− .00003135	21	+ 2.64725963	+ .21267387
2	+ 7.02217130	+ .00002694	22	+ 2.41700112	− .43674023
3	+ 6.79191280	− .00002095	23	+ 2.18674261	+ .49063145
4	+ 6.56165429	+ .00001284	24	+ 1.95648410	+ .04195061
5	+ 6.33139578	− .00000182	25	+ 1.72622559	− .43651651
6	+ 6.10113727	− .00001323	26	+ 1.49596708	− .22404767
7	+ 5.87087876	+ .00003397	27	+ 1.26570857	+ .09474711
8	+ 5.64062025	− .00006292	28	+ 1.03545006	+ .26322713
9	+ 5.41036174	+ .00010397	29	+ .80519155	+ .28286168
10	+ 5.18010323	− .00016337	30	+ .57493304	+ .23816634
11	+ 4.94984472	+ .00025153	31	+ .34467454	+ .17652451
12	+ 4.71958621	− .00038653	32	+ .11441603	+ .12333557
13	+ 4.48932770	+ .00060158	33	− .11584248	+ .08243897
14	+ 4.25906919	− .00096163	34	− .34610099	+ .05416555
15	+ 4.02881068	+ .00160407	35	− .57635950	+ .03489808
16	+ 3.79855217	− .00284834	36	− .80661801	+ .02239027
17	+ 3.56829367	+ .00552295	37	− 1.03687652	+ .01424526
18	+ 3.33803516	− .01202839	38	− 1.26713503	+ .00903156
19	+ 3.10777665	+ .02983246	39	− 1.49739354	+ .00574492
			40	− 1.72765205	+ .00359571

TABLE III
THE FILTER COEFFICIENTS AND THEIR ABSCISSA VALUES FOR VERTICAL COPLANAR LOOPS

K	η_k	C_k	K	η_k	C_k
0	+ 6.10113727	− .00001323	18	+ 1.95648410	+ .04195061
1	+ 5.87087876	+ .00003397	19	+ 1.72622559	− .43651651
2	+ 5.64062025	− .00006292	20	+ 1.49596708	− .22404767
3	+ 5.41036174	+ .00010397	21	+ 1.26570857	+ .09474711
4	+ 5.18010323	− .00016337	22	+ 1.03545006	+ .26322713
5	+ 4.94984472	+ .00025153	23	+ .80519155	+ .28286168
6	+ 4.71958621	− .00038653	24	+ .57493304	+ .23816634
7	+ 4.48932770	+ .00060158	25	+ .34467454	+ .17652451
8	+ 4.25906919	− .00096163	26	+ .11441603	+ .12333557
9	+ 4.02881086	+ .00160407	27	− .11584248	+ .08243897
10	+ 3.79855217	− .00284834	28	− .34610099	+ .05416555
11	+ 3.56829367	+ .00552295	29	− .57635950	+ .03489808
12	+ 3.33803516	− .01202839	30	− .80661801	+ .02239027
13	+ 3.10777665	+ .02983246	31	− 1.03687652	+ .01424526
14	+ 2.87751814	− .08103193	32	− 1.26713503	+ .00903156
15	+ 2.64725963	+ .21267387	33	− 1.49739354	+ .00574492
16	+ 2.41700112	− .43674023	34	− 1.72765205	+ .00359571
17	+ 2.18674261	+ .49063145	35	− 1.95791056	+ .00231841
			36	− 2.18816907	+ .00141123
			37	− 2.41842758	+ .00094868

ACKNOWLEDGMENT

Director, National Geophysical Research Institute, Hyderabad, India, has kindly authorized publication of this paper. M. Jayarama Rao assisted in preparation of the figures. N. Suresh Kumar typed the manuscript.

REFERENCES

[1] F. C. Frischknecht, "Fields about an oscillating magnetic dipole over a two-layer earth, and application to ground and airborne electromagnetic surveys," *Quarterly of the Colorado School of Mines*, vol. 62, no. 1, 1967.
[2] J. R. Wait, "Mutual electromagnetic coupling of loops over a homogeneous ground," *Geophysics*, vol. 20, no. 3, pp. 630–637, 1955.
[3] —, "Induction by an oscillating magnetic dipole over a two-layer ground," *Appl. Sci. Res.*, vol. 7, sec. B, pp. 73–80, 1958.
[4] A. Dey and S. H. Ward, "Inductive sounding of a layered earth with a horizontal magnetic dipole," *Geophysics*, vol. 35, no. 5, pp. 660–703, 1970.
[5] J. Ryu, H. F. Morrison, and S. H. Ward, "Electromagnetic fields about a loop source current," *Geophysics*, vol. 35, no. 5, pp. 862–896, 1970.
[6] J. Lajoie, J. Alfonso-Roche, and G. F. West, "E. M. response of an arbitrary source on a layered earth," *Geophysics*, vol. 40, no. 5, pp. 773–789, 1975.
[7] V. N. Starkhov, "Opredeleniye Osobikh loctek dvumernikh potentzial'nikh polei na osnove approksimatzii tzelimi analiticheskimi funktziyami eksponetzial'nogo tipa konochnoi stepeni," *Prikladnaya Geofizika*, no. 64, pp. 85–109, 1971.
[8] O. Koefoed, D. P. Ghosh, and G. J. Polman, "Computation of type curves for electromagnetic depth sounding with a horizontal transmitting coil by means of a digital linear filter," vol. 20, *Geophysical Prospecting*, pp. 406–420, 1972.
[9] R. K. Verma and O. Koefoed, "A note on the linear filter method of computing electromagnetic sounding curves," *Geophysical Prospecting*, vol. 21, pp. 70–76, 1973.
[10] R. K. Verma, "A feasibility study of electromagnetic depth sounding methods," D.Sc. dissertation, Delft University of Technology, Holland, 1973.
[11] Y. N. Kozulin, "A reflection method for computing the electromagnetic field above horizontal lamellar structures," *Izvestiya Academy of Sciences USSR*, Geophysics Series (English Edition), no. 3, pp. 267–273, 1963.
[12] W. L. Anderson, "FORTRAN IV programs for the determination of the transient tangential electric field and vertical magnetic field about a vertical magnetic dipole for an M-layer stratified earth by numerical integration and digital linear filtering," U.S. Geological Survey Rep. USGS-GD-73-017, PB-221240, 82 pp. 1973.
[13] —, "Electromagnetic fields about a finite element electric wire source," U.S. Geological Survey Rep. USGS-GD-74-041, PB-238-199/4 WC, 205 pp. 1974.
[14] —, "Improved digital filters for evaluating Fourier and Hankel transform integrals," U.S. Geological Survey Rep. USGS-GD-75-012, PB-242-800, 223 pp., 1975.
[15] —, "An optimal method for evaluating a class of convolution integrals with related kernels," *U.S. Geological Survey Rep.* USGS-GD-76-003, PB-251-156, 13 pp., 1976.

Characteristic Responses of Resistivity Tools in Elliptical Boreholes

STANLEY C. GIANZERO, MEMBER, IEEE

Abstract—**The solution for the potential created by a point-electrode current source in an elliptical borehole is obtained. This solution is applied to the computation of the responses of two typical shallow-investigation resistivity logging tools. These computations cover a range of contrasts between borehole-fluid and formation resistivities encompassing all cases normally encountered in well-logging practice. The effect of the finite size of the electrodes is approximately accounted for by first determining a circular borehole giving the same point-electrode resistivity response as the elliptical hole, and then making the same correction for electrode size to the elliptical-hole results as would apply in the circular-hole case.**

INTRODUCTION

IT IS WELL KNOWN from caliper measurements that well bores are often far from circular. Out-of-round holes may result from a number of different conditions, such as washed-out hole, bit wobble, hole caving, etc. In many cases these out-of-round holes are approximately elliptical in cross section.

It is reasonable to expect that the logging tools having the greater borehole effect will also be more affected by the out-of-roundness of the hole. By the same token, we should expect that resistivity tools having shallower depths of investigation will be more strongly influenced.

In analyses of the response of resistivity logging tools in boreholes, such as in [1], the well bore has been treated, as a first approximation, as if it were circular in cross section. In the present paper, a treatment will be described in which the well bore is taken to have an elliptical cross section. The necessary relationships will be developed to evaluate the influence of the elliptical shape of a well bore on responses of two typical shallow-investigation resistivity tools. The results will then be displayed, along with the data for circular holes, in borehole-correction charts of the form commonly employed by well-log analysts.

Manuscript received August 17; revised April 25, 1977.
The author is with Schlumberger-Doll Research Center, Ridgefield, CT.